Jahn-Teller Effect in the $^4T_{2g}$ Excited State of V^{2+} in MgO

M. D. STURGE
Bell Telephone Laboratories, Murray Hill, New Jersey
(Received 6 May 1965)

The lowest frequency ("no-phonon") line of the $^4A_2 \rightarrow {}^4T_2$ transition of V^{2+} in MgO is a doublet which can be split, shifted, and polarized by uniaxial stress. Both the zero-stress spectrum and the effect of stress are inconsistent with cubic symmetry in the $^4T_2$ state, or with a simple static Jahn-Teller effect. The major consequence of the Jahn-Teller effect is distortion along [100]-type axes, but in addition τ_{2g} vibrations play an important role. The data can be fitted with an effective Hamiltonian which contains terms of T_{2g} symmetry. These terms mix the three vibronic states corresponding to the three possible directions of static distortion. The resulting vibronic energy levels form a singlet and a doublet, the latter lying lower. We can calculate the effect of stress quantitatively, using the one-electron matrix elements of strain found by experiments on the ^2E state (which shows no Jahn-Teller effect), and obtain excellent agreement with experiment. A tentative explanation of the effective Hamiltonian in terms of more fundamental concepts is suggested.

1. INTRODUCTION

THE Jahn-Teller theorem[1,2] states that a system of interacting electrons and nuclei in a degenerate electronic state is unstable, since the system can always reduce its energy by distorting in such a way as to remove the degeneracy in first order. There are only two exceptions: Kramers degeneracy cannot be removed by any distortion; and for certain states of a linear molecule there is no distortion which removes the degeneracy in first order. The latter case is obviously of no interest in solids.

The linear reduction in energy due to the removal of degeneracy will ultimately be balanced by the (initially quadratic) increase in elastic energy[3] and a new position of equilibrium will be reached in which there is a permanent distortion of the system. Removal of the orbital degeneracy of a transition-metal ion can reduce the energy by 100 to 10 000 cm^{-1}, whereas removal of the spin degeneracy of an orbital singlet well-separated from other states only reduces the energy by 0.1–10 cm^{-1}, much less than the typical zero-point energy of vibration.[2,4] It follows that spin degeneracy can usually be ignored in consideration of the Jahn-Teller effect. Furthermore, sufficiently strong spin-orbit coupling, by removing degeneracy, can in many cases stabilize a symmetric situation against Jahn-Teller distortion.[5]

We will consider in this paper the case of a transition-metal ion in octahedral-oxygen coordination. The ground states of such systems have been widely studied by spin resonance, and the Jahn-Teller effect has frequently been observed.[6–8] The distorted structures of cupric, manganic, and chromous compounds have also been interpreted in terms of the Jahn-Teller effect.[9,10] It turns out that in all the cases where the Jahn-Teller effect has incontrovertibly been observed there is a single hole or electron in an e orbital, any t_2 orbitals being empty, half-filled, or filled, so that the ground state has E symmetry.[11] Besides the classic case of Cu^{2+},[6,9,10] cases in point are Ni^+,[8] Ni^{3+}, Pt^{3+},[7] Mn^{3+},[12] and probably Cr^{2+}.[9,10] Such ions as Co^{2+} and Fe^{2+}, whose ground

[1] H. A. Jahn and E. Teller, Proc. Roy. Soc. (London) **A161**, 220 (1937).
[2] H. A. Jahn, Proc. Roy. Soc. (London) **A164**, 117 (1938).
[3] J. H. Van Vleck, J. Chem. Phys. **7**, 72 (1939).
[4] V. I. Avvakumov, Opt. i Spektroskopiya **13**, 588 (1962) [English transl.: Opt. Spectry. (USSR) **13**, 332 (1962)], argues that even quite weak Jahn-Teller effects, ~0.1 cm^{-1}, can be important in spin resonance. There seems to be no experimental evidence for this.
[5] U. Öpik and M. H. L. Pryce, Proc. Roy. Soc. (London) **A238**, 425 (1957).
[6] B. Bleaney, K. D. Bowers, and R. S. Trenam, Proc. Roy. Soc. (London) **A228**, 157 (1955); J. W. Orton, P. Auzins, J. H. E. Griffiths, and J. E. Wertz, Proc. Phys. Soc. (London) **78**, 554 (1961).
[7] S. Geschwind and J. Remeika, J. Appl. Phys. **33**, 370 (1962).
[8] W. Hayes and J. Wilkens, Proc. Roy. Soc. (London) **A281**, 340 (1964).
[9] J. D. Dunitz and L. E. Orgel, J. Phys. Chem. Solids **3**, 20 (1957); J. B. Goodenough and A. L. Loeb, Phys. Rev. **98**, 391 (1955). For a review of the data and for further references see A. D. Liehr, J. Phys. Chem. **67**, 389 (1963); N. S. Ham, Spectrochim. Acta **18**, 775 (1962); and J. B. Goodenough, *Magnetism and the Chemical Bond* (Interscience Publishers, Inc., New York, 1963). Much of the structural evidence for a static Jahn-Teller effect in pure compounds is open to the objection that packing considerations can force a low symmetry regardless of the electronic degeneracy of the ion. On the other hand, loss of symmetry on excitation from a non-degenerate ground state to a degenerate excited state, such as is described in the present paper, can be explained only by the Jahn-Teller effect.
[10] A. D. Liehr and C. J. Ballhausen, Ann. Phys. (N. Y.) **3**, 304 (1958).
[11] D. S. McClure [J. Chem. Phys. **36**, 2757 (1962)] has interpreted the anomalous polarization of the vibrational structure of the $^3T_1 \rightarrow {}^3T_2$ absorption band of V^{3+} in Al_2O_3, and of the $^4A_2 \rightarrow {}^4T_2$ band of Cr^{3+}, in terms of a static Jahn-Teller effect in the excited (T_2) states of these ions. I. B. Bersuker and B. G. Vekhter, Fiz. Tverd. Tela **5**, 2432 (1963) [English transl.: Soviet Phys.—Solid State **5**, 1772 (1964)] have discussed the anomalous g factors observed in the ground state of Ti^{3+} in terms of a temperature-dependent dynamic Jahn-Teller effect. In both these cases a t_2 electron is involved, but there are difficulties about the latter author's approach [see F. S. Ham, Phys. Rev. **138**, A1727 (1965)] and it is doubtful if interpretation in terms of the Jahn-Teller effect is the only explanation of the data. Structural evidence for a static Jahn-Teller effect in tetrahedrally coordinated Cu^{2+} and Ni^{2+}, which have t_2 holes in the ground state, is presented by R. J. Arnott, A. Wold, and D. B. Rogers, J. Phys. Chem. Solids **25**, 161 (1964).
[12] D. B. Fraser, E. M. Gyorgy, R. C. LeCraw, J. P. Remeika, F. J. Schnettler, and L. G. Van Uitert, J. Appl. Phys. **36**, 1016 (1965).

states have T-type (threefold) orbital symmetry, do not show Jahn-Teller distortion in spin resonance.[13] The reason for this is basically that spin-orbit coupling is important in T states. Spin-orbit coupling removes the orbital degeneracy and leaves either a singlet, a Kramers doublet (as in Co^{2+}), or a state which, while still degenerate, may be a nearly pure spin triplet (Fe^{2+}). More subtle reasons why spin-orbit coupling will nearly always suppress the more dramatic consequences of the Jahn-Teller effect are discussed by Ham[14] (see below).

One of the reasons for studying the Jahn-Teller effect in excited states rather than in ground states is that there is a much wider choice of states available. Furthermore, the existence of states within the same system which do not show the Jahn-Teller effect can clarify the situation by providing, so to speak, a reference point for those states which do show the effect. For instance, study of the $^3T_2$ excited state of Ni^{2+} in MgO, which shows no Jahn-Teller distortion at all,[15,16] has produced evidence for the effects discussed by Ham.[14,16]

The case of V^{2+} in MgO to be discussed in this paper is of particular interest because the data can only be explained in terms of a Jahn-Teller effect, but the effect takes a different form from that predicted by naive application of the Jahn-Teller theorem, or by the more sophisticated analysis of Ham.[14] The way the Jahn-Teller effect operates in this case, though not yet fully understood, may cast some light on the general problem of triply degenerate states in cubic or nearly cubic crystals.

In the next section the consequences of the Jahn-Teller effect, as they appear in the optical-absorption spectrum of a transition-metal ion, are discussed in a general way. Section 3 describes the experiment, in which the Jahn-Teller distorted $^4T_2$ state of V^{2+} is split by a uniaxial stress applied along various crystallographic directions. Section 4 is devoted to demonstrating that the results of this experiment are inconsistent with the assumption that cubic symmetry is retained in the excited state, and can only be explained in terms of a Jahn-Teller effect. Section 5 discusses the static Jahn-Teller effect, and Ham's treatment of the dynamic effect, and shows that the data cannot be explained in terms of existing theory, which treats interaction with only one type of lattice distortion (ϵ_g or τ_{2g}) at a time. Section 6 sets up a simple effective Hamiltonian which describes the data empirically; from it we can derive the observed energy levels and relative transition probabilities with remarkable accuracy, using only one adjustable parameter. Section 7 attempts to justify this effective Hamiltonian in terms of more fundamental concepts. Interaction with both ϵ_g and τ_{2g} distortions is taken into account but only in an *ad hoc* and rather intuitive manner. In conclusion, it is pointed out that the effective Hamiltonian of Sec. 6 could be the starting point for a full theoretical treatment of the Jahn-Teller effect in an octahedrally coordinated ion.

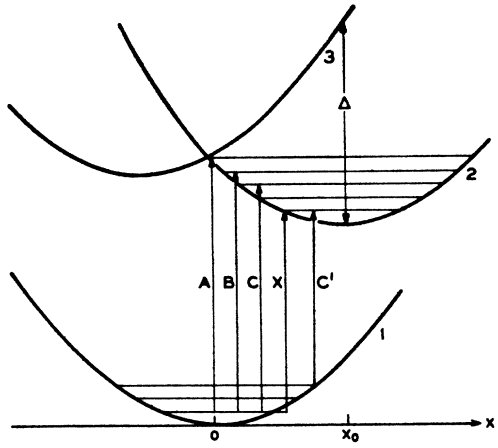

FIG. 1. Configuration coordinate diagram for a center with a nondegenerate ground state and a triply-degenerate electronic excited state. The abscissa may represent any axial distortion which splits the excited state in first order; the ordinate is the energy of the combined electron-nuclear system. Δ is the splitting between the singlet and the doublet at the equilibrium distortion x_0.

2. THE JAHN-TELLER EFFECT IN OPTICAL ABSORPTION

How does one study the Jahn-Teller effect in excited electronic states? Application of the Franck-Condon principle might lead one to reject absorption spectroscopy as a technique, because the nuclear configuration cannot change at the moment of transition.[17] This, however, is too naive.[18] Consider a system with a nondegenerate ground state, and plot its energy as a function of some distortion coordinate x (Fig. 1).[19] In general, the potential energy of the combined electron-nuclear system in the electronic ground state will follow curve 1, a parabola centered on $x=0$. The horizontal lines represent vibrational levels of the system. Now consider a degenerate excited state, for definiteness triply degenerate, which splits into a doublet and a singlet under the distortion x. Then the energy of the system in the electronic singlet state follows curve 2, with its own vibrational levels. Curve 3 represents the energy in the electronic doublet state. Unless the lattice potential is highly anharmonic, the turning point in curve 2 is an absolute minimum for the

[13] W. Low, Phys. Rev. **109**, 256 (1958); W. Low and M. Weger, *ibid.* **118**, 1119 (1960); J. H. Van Vleck, Physica **26**, 544 (1960).
[14] F. S. Ham, Phys. Rev. **138**, A1727 (1965).
[15] R. Pappalardo, D. L. Wood, and R. C. Linares, J. Chem. Phys. **35**, 1460 (1961); see also J. Ferguson, H. J. Guggenheim, and D. L. Wood, J. Chem. Phys. **40**, 822 (1964).
[16] M. D. Sturge (to be published).
[17] J. Franck, Trans. Faraday Soc. **21**, 536 (1926); E. U. Condon, Phys. Rev. **32**, 858 (1928); M. Lax, J. Chem. Phys. **20**, 1752 (1952).
[18] H. Sponer and E. Teller, Rev. Mod. Phys. **13**, 75 (1941).
[19] A. von Hippel, Z. Physik **101**, 680 (1936); F. Seitz, Trans. Faraday Soc. **35**, 74 (1939).

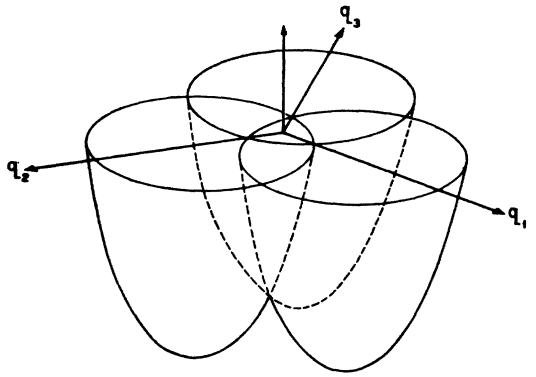

FIG. 2. Potential surfaces for a T state in Q_2Q_3 space [after A. D. Liehr, J. Phys. Chem. **67**, 389 (1963)]. The nonorthogonal coordinates q_1, q_2, and q_3 are defined in Table I(b). Each of the three paraboloids is associated with a definite electronic substate; for instance, the paraboloid with its minimum along the q_1 axis is associated with $|T_1x\rangle$ or $|T_2\xi\rangle$. The paraboloids have been drawn as surfaces of revolution for clarity; in general this is not correct and a horizontal section would reveal ellipses rather than circles.

excited electronic state (the apparent minimum of curve 3 in Fig. 1 is really only a cusp; see Fig. 2, of which Fig. 1 is a vertical section). The displacement x_0 of the singlet minimum represents the equilibrium ("static") Jahn-Teller distortion, at which the singlet-doublet splitting is Δ. The Franck-Condon principle states that only vertical transitions in Fig. 1 are possible. The most probable absorptive transition at low temperature is that marked A, as the most probable value of x in the ground state is zero; but transitions B, C, etc. are also possible with steadily decreasing probability. In particular, if x_0 is not too large, transition X, which connects the lowest vibrational states of curves 1 and 2, has appreciable intensity, and is known as the 0-0 or no-phonon line.[20] Note that this transition reflects not only the symmetry of the nuclear configuration in the ground state but also that in the distorted excited state.

TABLE I. Distortion coordinates for the octahedron.

(a) Transformation properties of the even-parity normal coordinates

Van Vleck notation	Transforms as	O_h Rep
Q_1	$x^2+y^2+z^2$	A_{1g}
Q_2	$\sqrt{3}(x^2-y^2)$	E_g
Q_3	$2z^2-x^2-y^2$	
Q_4	yz	T_{2g}
Q_5	zx	
Q_6	xy	

(b) Relationship of the nonorthogonal coordinates q to Q_2, Q_3

$q_1=-\frac{1}{2}Q_3+\frac{1}{2}\sqrt{3}Q_2$, transforms as $2x^2-y^2-z^2$
$q_2=-\frac{1}{2}Q_3-\frac{1}{2}\sqrt{3}Q_2$, transforms as $2y^2-z^2-x^2$
$q_3=Q_3$ transforms as $2z^2-x^2-y^2$

[20] E. O. Kane, Phys. Rev. **119**, 40 (1960); D. E. McCumber, Phys. Rev. **135**, A1676 (1964).

There are many distortions of the octahedron which x might represent. The totally symmetric α_{1g} distortion, while producing no splitting, can produce a first-order shift even on a nondegenerate level, and its effect on the energy levels can be represented by Fig. 1 in which curve 3 is omitted. The other five even distortions of the octahedron, two ϵ_g and three τ_{2g} distortions, in general give first order splittings of a triply degenerate state; it has been shown by Öpik and Pryce[5] that in the harmonic approximation they act independently and give minima corresponding to distortions along [001] and [111] type axes, respectively. Odd distortions of the octahedron (τ_{1u} and τ_{2u}) can only produce a Jahn-Teller effect if there is a near degeneracy of odd- and even-parity electronic states[5]; this may be the case in the F center in alkali halides but does not normally occur in transition-metal ions in insulating crystals. It may be objected that in a crystal there are a large number of possible distortions besides those of the nearest-neighbor octahedron. However, insofar as nearest-neighbor interactions will be stronger than all others, only the distortions of the octahedron will be involved in the Jahn-Teller effect, which automatically selects that distortion which produces the largest splitting of the degenerate electronic state. Any distortion of the octahedron can be described in terms of its normal coordinates, α_{1g}, ϵ_g, τ_{2g}, etc. The fact that these coordinates do not correspond to normal modes of the lattice is irrelevant, except insofar as the "modes" associated with the coordinates do not have a definite frequency, but are spread throughout the phonon spectrum.

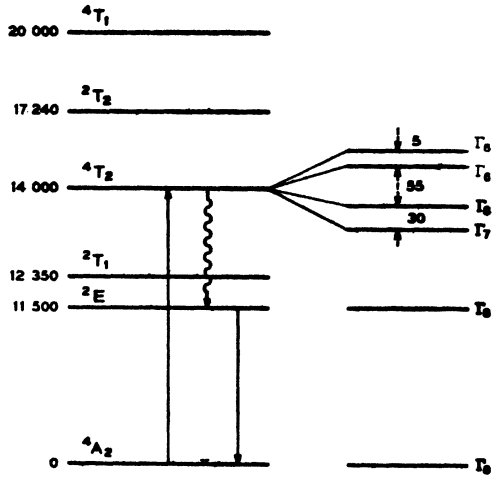

FIG. 3. The lower energy levels of V^{2+} (d^3 configuration) in a cubic field. Mulliken notation is used for orbital states without spin-orbit coupling, Bethe notation for the spin-orbital states. The frequencies on the left are experimental [M. D. Sturge, Phys. Rev. **130**, 639 (1963)] but the splittings on the right are calculated by computer diagonalization [A. D. Liehr, J. Phys. Chem. **67**, 1314 (1963)] of the complete matrices [J. C. Eisenstein, J. Chem. Phys. **34**, 1628 (1961)] for the d^3 configuration in a cubic field, with the parameters of Sturge (*op. cit.*).

It turns out experimentally that the ϵ_g distortion is dominant in most cases. The minima correspond to tetragonal distortions along cube directions.[5] Three distortion coordinates q_1, q_2, and q_3, corresponding to the three directions of distortion, are defined in terms of the normal coordinates of the octahedron Q_2 and Q_3 (Van Vleck's notation[3]) in Table I. The potential surfaces for an electronic T state in Q_2, Q_3 space are shown in Fig. 2.[21,22] Spin-orbit coupling is neglected in this figure. If it is weak compared with the Jahn-Teller energy it will have no important effect (except near the central point of maximum degeneracy). This is the case for the $^4T_2$ state of V^{2+} to be discussed in this paper. If the spin-orbit coupling is very strong, and the number of electrons is even, the states can still be classified as A, E, and T states and the same analysis applies.

Note that in Q_2,Q_3 space there is no possibility of tunnelling from one potential well to another; this is because the singlet electronic states corresponding to each well are orthogonal to one another, even in the presence of tetragonal distortion.[23] Thus one might expect always to see a static Jahn-Teller effect, at any rate so long as the depth of each well is greater than the zero-point energy of vibration. In an important paper Ham[14] has shown that this is not correct. Even though the electronic wave functions are orthogonal, the vibrational wave functions overlap somewhat in Q_2,Q_3 space. If this overlap is significant, spin-orbit coupling, which connects electronic states in different valleys, will not be completely quenched. Under most circumstances the anisotropy characteristic of the static Jahn-Teller effect will not be seen, though there is an over-all reduction in the matrix elements of all operators, such as orbital momentum, which connect the electronic states in first order.

The situation in T states is very different from that of a doubly degenerate E electronic state,[24] for in the latter case there is no first order spin-orbit coupling. On the other hand, the electronic states corresponding to the three directions of distortion are themselves not orthogonal; the potential barriers separating neighboring wells can be quite low, and transitions between the wells occur readily. The anisotropy characteristic of the static Jahn-Teller effect can then be averaged out even in the absence of external perturbation, and the threefold degeneracy of the ground state (corresponding to the three possible directions of distortion) is raised, leaving a doublet lowest. This is known as the dynamic Jahn-Teller effect. It is the purpose of this paper to show that the $^4T_2$ state of V^{2+} shows a rather similar mixing of Jahn-Teller distortions characteristic of the dynamic effect. The data cannot be explained in terms of Ham's analysis, and the τ_{2g} vibrations play an essential role.

A note on nomenclature is in order. I use the term "static Jahn-Teller effect" to refer to a permanent local distortion in the environment of an ion, producing anisotropy observable (for instance) in the spin resonance spectrum. By the "dynamic Jahn-Teller effect" I mean the case where the several equivalent distortions are mixed, by tunnelling or otherwise, so that the original symmetry (cubic in the present case) is restored. The properties of the system may be drastically affected by the dynamic Jahn-Teller effect but the local (time-averaged) symmetry is still cubic. This usage agrees with that of Ham.[14]

3. EXPERIMENTAL MEASUREMENTS

MgO has the NaCl structure and V^{2+} substitutes for Mg^{2+}, occupying a site of perfect cubic symmetry, as is shown by spin resonance.[25] The lower electronic energy levels of V^{2+} in a cubic field[26] are shown in Fig. 3. For the reasons given in Ref. 26 it is difficult to measure the absorption spectrum directly. However, V^{2+} shows strong sharp line fluorescence at 11 500 cm^{-1} due to the $^2E \rightarrow {}^4A_2$ transition, and it has been shown[26,27] that the excitation spectrum of this fluorescence (i.e., the strength of fluorescence under monochromatic excitation, measured as a function of exciting wavelength) gives an accurate picture of the absorption spectrum. Polarized excitation spectra were taken at temperatures from 20°K upwards, with a Bausch and Lomb $f/4.4$ grating monochromator which has a resolution of 5–10 cm^{-1}.

That part of the excitation spectrum which is due to the $^4A_2 \rightarrow {}^4T_2$ transition is shown in Fig. 4. The doublet XY is the no-phonon line. This is shown by its magnetic dipole character (to be demonstrated later). As the octahedral site of MgO has a center of symmetry, a purely electronic transition with in the d^n configuration can only be magnetic dipole (or electric quadrupole; this has never been observed in terrestrial spectra).

[21] W. Moffitt and W. Thorsen, Phys. Rev. **108**, 1251 (1957).
[22] A. D. Liehr, J. Phys. Chem. **67**, 389 (1963).
[23] A symmetry argument due to M. H. L. Pryce (private communication) demonstrates this point as follows. The three electronic states transform either as x,y,z or as yz,zx,xy. Whichever is the axis of tetragonal distortion, all three cube axes remain twofold axes of symmetry. A 180° rotation changes the sign of two of the states while leaving the third unchanged. Thus the states are orthogonal even in presence of the tetragonal distortion.
[24] H. C. Longuet-Higgins, U. Öpik, M. H. L. Pryce, and R. A. Sack, Proc. Roy. Soc. (London) **244**, 1 (1958); V. I. Avvakumov, Zh. Experim. i Teor. Fiz **37**, 1017 (1959) [English transl.: Soviet Phys.—JETP **10**, 723 (1960)]; M. S. Child and H. C. Longuet-Higgins, Phil. Trans. Roy Soc. London **254**, 259 (1961); M. C. M. O'Brien, Proc. Roy. Soc. (London) **281**, 323 (1964).
[25] J. S. van Wieringen and J. G. Rensen, *Proceedings of the First International Conference on Paramagnetic Resonance Jerusalem, 1962* (Academic Press Inc., New York, 1963), p. 105. F. R. Merritt (private communication) has measured the spin-resonance spectrum due to V^{2+} in the heat-treated MgO used in the present experiment. The spectrum is purely cubic and is essentially the same as that observed by van Wieringen and Rensen, but the lines are somewhat broader. Any deviation from cubic symmetry produces a ground-state splitting of less than 5×10^{-4} cm^{-1}.
[26] M. D. Sturge, Phys. Rev. **130**, 639 (1963).
[27] R. E. Weber, L. C. Hall, and J. E. Wertz, Bull. Am. Phys. Soc. **9**, 706 (1964).

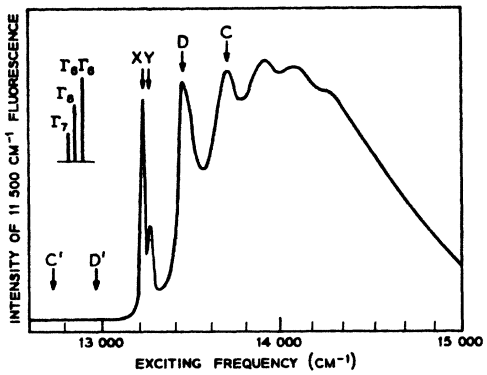

FIG. 4. The $^4A_2 \rightarrow {}^4T_2$ absorption band of V^{2+} in MgO, as it appears in the excitation spectrum of the 11 500 cm^{-1} fluorescence at 20°K. The vertical scale is arbitrary. Insert is the predicted "no-phonon line" in the absence of Jahn-Teller effects.

On the other hand we would expect that electric-dipole transitions, induced by odd modes of the octahedron and of the lattice (a general phonon always has some odd character), will usually be dominant in the vibronic (vibrational-electronic) transitions. Further evidence that XY is the no-phonon line is the appearance at temperatures above 100°K of broad lines ("hot bands") at C' and D', where $CX \approx XC', DX \approx XD'$, and the strengths of C' and D' are related to those of C and D by the appropriate Boltzmann factor. Lines C' and D' correspond to transitions from excited vibrational levels of the ground electronic state. (See Fig. 1.)

As the temperature is raised the lines broaden, the width of the stronger no-phonon line increasing from 20 cm^{-1} at 20°K to 28 cm^{-1} at 77°K and rapidly above this temperature.[28] The splitting of the doublet is independent of temperature up to 112°K, above which it is not resolved. The spectrum is independent of V^{2+} concentration (which is always less than ~0.1%) and of the detailed heat treatment.

The first evidence that the $^4T_2$ state has lost its cubic symmetry is given in Fig. 4. If the situation were cubic the $^4T_2$ state would be split by spin-orbit coupling as shown on the right in Fig. 3, and the no-phonon line would split as shown in the insert in Fig. 4 (the Γ_6 and Γ_8 states, which are only split in second order, would not be resolved). The prediction is clearly inconsistent with observation.

To proceed further it is necessary to perturb the levels in some way in order to determine their symmetry. The Zeeman effect is the obvious choice, but unfortunately the no-phonon line is too broad to be split in obtainable magnetic fields. The line can, however, be split by uniaxial stress, and this is the method used here. The one-electron matrix elements of stress can be determined from the stress splitting of the ^2E state,[29] which is known to be cubic.[26,30] Thus it is possible to calculate the entire stress splitting pattern without any adjustable parameters, on the hypothesis that the situation in zero stress is cubic. This is done in the next section.

The specimens for stress measurements were rectangular prisms a few mm long and 3–5 mm^2 in cross section. The ends and sides were aligned within 1° of the required crystallographic axes (to within 20′ in the case of the [001] and [111] specimens). The specimens were stressed in an apparatus similar to that described by Schawlow *et al.*[31]; they usually broke at about 45 kg/mm^2 but showed signs of permanent damage (birefringence) after stressing above 40 kg/mm^2. The specimens were prepared by the methods described in Ref. 26 and were somewhat cloudy. The consequent scattering caused some depolarization of the exciting light.

The magnetic-dipole character of the transition under study was demonstrated by stressing along the [110] axis, and taking spectra with four possible combinations of polarizations, as shown in Fig. 5. The coincidence of the two spectra with H parallel to the stress and the large discrepancy between the two with E parallel to the stress show that at least 90% of the intensity is a consequence of magnetic-dipole transitions.

4. CALCULATIONS ON THE ASSUMPTION OF CUBIC SYMMETRY

The splitting of the ^2E state under a compressive stress P along [001] is[31]

$$\Delta_{001}=\frac{2P}{c_{11}-c_{12}}\left[b^2\langle e\|u^E\|e\rangle+\frac{4bc}{\sqrt{3}}\langle t_2\|u^E\|t_2\rangle\right], \quad (1)$$

while the splitting for a [111] stress is[31]

$$\Delta_{111}=\frac{4P}{(\sqrt{6})c_{44}}\frac{\zeta\langle t_2\|u^{T_2}\|t_2\rangle}{W(^2T_2)-W(^2E)} \quad (2)$$

and for a [110] stress

$$\Delta_{110}=(\tfrac{1}{4}\Delta_{001}^2+\tfrac{1}{3}\Delta_{111}^2)^{1/2}. \quad (3)$$

Here the reduced ("double-barred") matrix elements represent the effect of a unit strain of E or T_2 symmetry on the e and t_2 orbitals; b and c are configuration mixing coefficients defined in Ref. 31 and evaluated for V^{2+} in Ref. 29; ζ is the spin-orbit coupling parameter; and $W(\Gamma)$ is the energy of the state Γ (see Fig. 3). The elastic constants c_{11}, c_{12}, and c_{44} cancel out in the final comparison with experiment; if actual values are

[28] The temperature dependence of the linewidth is of intrinsic interest, but is not directly relevant to the problem of the Jahn-Teller effect, and will be discussed in a separate publication.

[29] M. D. Sturge, Phys. Rev. **131**, 1456 (1963).

[30] The ^2E state derives from the half-filled shell t_2^3 and its stress splittings are very small. Any Jahn-Teller effect will therefore also be small and easily overcome by the zero-point energy of vibration.

[31] A. L. Schawlow, A. H. Piksis, and S. Sugano, Phys. Rev. **122**, 1469 (1961).

needed for comparison with a theoretical model (such as the point-charge model used in Ref. 31) no significant error is introduced by using the room-temperature values.[32]

It turns out that whereas $\langle t_2\|u^{T_2}\|t_2\rangle$ is sufficient to determine the splitting of $^4T_2$ under [111] stress, we need a combination of $\langle e\|u^E\|e\rangle$ and $\langle t_2\|u^E\|t_2\rangle$ different from that of Eq. (1) in order to calculate the splitting of $^4T_2$ under [001] stress. Thus we need, besides the experimental data Δ_{001} and Δ_{111}, an independent value for $\langle t_2\|u^E\|t_2\rangle/\langle e\|u^E\|e\rangle$. Here we can make use of the fortunate fact that for both V^{2+} and the isoelectronic Cr^{3+} the matrix elements calculated from the point-charge model,[31] using Hartree-Fock wave functions[33] for the central ion, give excellent agreement with the observed splittings.[29] Thus it is reasonable to use the point-charge model to calculate $\langle e\|u^E\|e\rangle$ and $\langle t_2\|u^E\|t_2\rangle$ independently.[34]

In calculating the stress splittings we neglect the effect of states other than $^4T_2$; that is, we use first-order perturbation theory with strong-field wave functions.[35] This can easily be justified for the cubic situation by working out typical second-order terms such as

$$\frac{\langle {}^4T_2|\,\mathbf{L}\cdot\mathbf{S}\,|{}^4T_1\rangle\langle {}^4T_1|\,U^E\,|{}^4T_2\rangle}{W({}^4T_1)-W({}^4T_2)},$$

whose contribution turns out to be less than 2% of the first-order term. There are no other $^4T_2$ states in d^3, so we need not worry about configuration mixing by the Coulomb interaction.

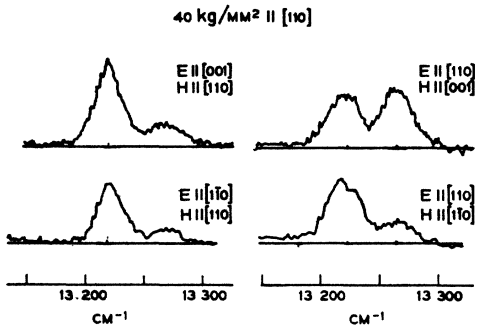

FIG. 5. Effect of a stress of 40 kg/mm², applied parallel to [110], on the nonphonon doublet at 77°K. The four polarizations are chosen to demonstrate the magnetic-dipole character of the transition. If it were electric dipole, the two spectra on the right would be identical while those on the left would differ.

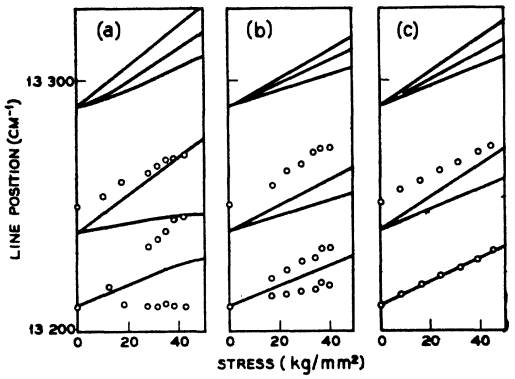

FIG. 6. Experimental positions of absorption peaks in the no-phonon multiplet of the $^4A_2 \rightarrow {}^4T_2$ transition at 20°K, as a function of stress applied in various crystallographic directions; the full lines are the predictions of Sec. 4, which are based on the assumption that there is cubic symmetry in the excited state in the absence of a stress: (a) stress parallel to [001]; (b) stress parallel to [110]; (c) stress parallel to [111].

The methods and tables of Refs. 36 and 37 were used to calculate the energy levels and wave functions. The splittings are expressed in terms of three parameters, ζ, u, and v. The one-electron spin-orbit coupling parameter ζ was found in other experiments[26] to be between 110 and 140 cm^{-1} and taken here to be 120 cm^{-1}. The tetragonal splitting parameter, $u=\frac{3}{4}\langle e\|u^E\|e\rangle - \frac{1}{2}\sqrt{3}\langle t_2\|u^E\|t_2\rangle$, is found to be -0.84 $cm^{-1}/kg\ mm^{-2}$ in compression (see above)[38]; and the trigonal splitting parameter $v=(\sqrt{\frac{3}{2}})\langle t_2\|u^T2\|t_2\rangle$, is -0.50 $cm^{-1}/kg\ mm^{-2}$.

The energy levels move under stress as shown by the solid lines in Fig. 6.[39] The circles in Fig. 6 represent the positions of the observed absorption peaks. The relative strengths of the lines can be calculated from the wave functions by summing appropriately over $\langle {}^4A_2M_s|\,L_0\,|{}^4T_2M_s\theta\rangle$ for $H\|p$ and $\langle {}^4A_2M_s|\,L_\pm\,|{}^4T_2M_s\theta\rangle$

[32] *American Institute of Physics Handbook*, edited by D. E. Gray (McGraw-Hill Book Company, Inc., New York, 1963), 2nd ed., p. 2–52; M. A. Durand, Phys. Rev. **50**, 449 (1936).

[33] R. E. Watson, M.I.T., Solid State and Molecular Theory Group, Technical Report No. 12, 1959 (unpublished).

[34] A word of caution is necessary here. Each matrix element for [001] stress is given by the point-charge model in terms of two quantities $B_2\langle r^2\rangle$ and $B_4\langle r^4\rangle$, where the B's describe the lattice potential and the $\langle r^n\rangle$ are determined from the electronic wave functions of the central ion. It turns out that the $\langle r^2\rangle$ term dominates the ^2E splitting under [001] strain, while it cancels out of the $^4T_2$ splitting. Another way to get the $\langle r^4\rangle$ term alone, without having to assume a central ion wave function at all, is to use the Bethe formula [H. A. Bethe, Ann. Physik **3**, 133 (1929)] relating $\langle r^4\rangle$ to the observed cubic field splitting 10 Dq. This method gives a $^4T_2$ splitting about twice as great as that found using Hartree-Fock wave functions (that is, 10 Dq is twice what is calculated from Hartree-Fock, while it is roughly a factor of 4 *less* than that calculated from Slater wave functions) and points up the limitations of the point-charge model. The approach here is to use the point charge model as a parametrization scheme to describe the effects of stress, which it does extremely successfully, without delving into its validity as a description of the actual physical situation.

[35] S. Sugano and Y. Tanabe, J. Phys. Soc. Japan **13**, 880 (1958).

[36] Y. Tanabe and H. Kamimura, J. Phys. Soc. Japan **13**, 394 (1958).

[37] J. S. Griffith, *The Irreducible Tensor Method for Molecular Symmetry Groups* (Prentice Hall Inc., Englewood Cliffs, New Jersey, 1962).

[38] Reducing the ratio $\langle t_2\|u^E\|t_2\rangle/\langle e\|u^E\|e\rangle$ from its point charge value of 0.6 to a more realistic value of (say) 0.3 only increases $|u|$ by 50%. Such an increase would not affect the conclusions of this or subsequent sections.

[39] A shift to higher energy of all levels, linear with stress, has been included to allow for the hydrostatic (α_{1g}) component of strain. This shift was calculated by taking the data on the shift of the $^4T_2$ band maximum of $MgO:Cr^{3+}$ under hydrostatic stress [S. Minomura and H. G. Drickamer, J. Chem. Phys. **35**, 903 (1961)] and scaling it to $MgO:V^{2+}$, assuming that the relative change in 10 Dq will be the same for both ions. The shift is 0.5 $cm^{-1}/kg\ mm^{-2}$, independent of direction of the stress.

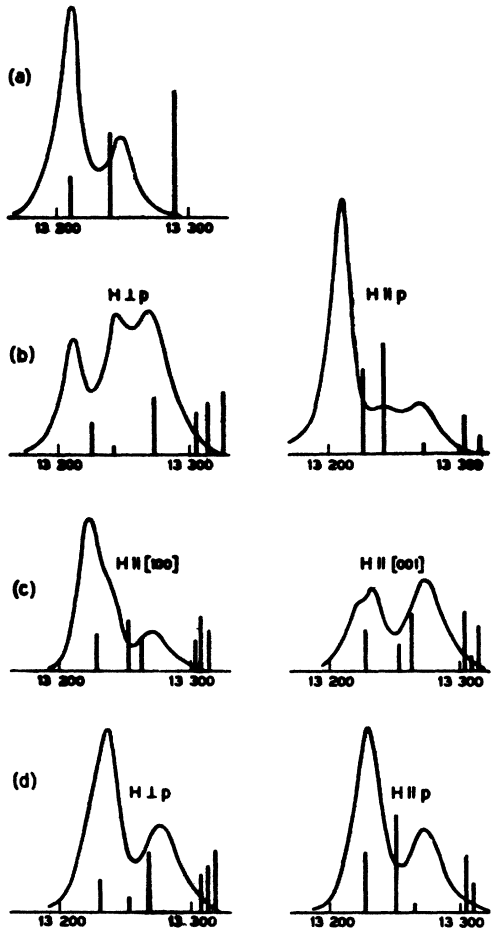

FIG. 7. Spectrograms of the $^4A_2 \rightarrow {}^4T_2$ no-phonon transition for a stress in various directions, compared with the relative (magnetic dipole) line strengths predicted by the theory of Sec. 4 (vertical lines). The polarization is given in terms of the H vector on each spectrogram. (a) zero stress (unpolarized); (b) 42 kg/mm² parallel to [001]; (c) 40 kg/mm² parallel to [110]; (d) 44 kg/mm² parallel to [111].

for $H \perp p$. The splitting of the $^4A_2$ ground state under stress is extremely small (less than 10^{-2} cm^{-1} at 40 kg/mm² [40]) and can be neglected. Some predicted line patterns are compared with the observed spectra in Fig. 7.

It is clear that the data cannot be fitted by this theory. First, we note that experimentally there is no over-all polarization induced by stress. This shows that we are looking at the entire $^4T_2$ state and not just some components of it. If (for instance) the transition to $\Gamma_6\Gamma_8$ were for some reason broadened beyond observation, these states would still mix with the observed states and produce approximately 50% polarization at the maximum stress. No such polarization is observed, the limit of observation being about 10%. We also note that the wrong line splits under [001] stress. Most significant of all, under [111] stress no splitting or polarization is observed at all. The predicted splitting (which is independent of the point-charge or any other model) would be quite large enough to see. We can safely conclude that the symmetry in the $^4T_2$ state is lower than cubic; the state has "lost O_h."

[40] E. Feher, Bull. Am. Phys. Soc. **10**, 699 (1965).

5. STATIC JAHN-TELLER EFFECT

The observation that [111] stress has no effect apart from a general shift in the spectrum immediately suggests a static Jahn-Teller effect, with distortion along [001]-type axes. This is, of course, what we originally predicted, the relative values of u and v being such that tetragonal (ϵ_θ) distortion is preferred over trigonal ($\tau_{2\theta}$). On average $\frac{1}{3}$ of the ions will distort along each of the cube directions. The distortion will presumably be compression, which brings the singlet component of T_2 lowest[41]; thus the $|{}^4T_2\xi\rangle$ state will be associated with distortion along the x axis [100], $|{}^4T_2\eta\rangle$ with [010] distortion, $|{}^4T_2\zeta\rangle$ with [001] distortion. Note that these wave functions are real and can therefore have no first-order spin-orbit splitting. If the Jahn-Teller splitting is Δ (Fig. 1), the second-order spin-orbit splitting is $\zeta^2/18\Delta$, and if Δ is of the order of the bandwidth (1000 cm^{-1})[42] the splitting due to this cause is less than 1 cm^{-1} (Δ would have to be greater than a typical zero-point vibrational energy $\frac{1}{2}\hbar\omega_\epsilon$, say 100 cm^{-1}, for there to be a static Jahn-Teller effect at all, so the most the second order spin-orbit splitting can be is 8 cm^{-1}). Thus the static Jahn-Teller effect cannot explain the observed 40 cm^{-1} splitting in zero stress. This splitting is independent of concentration. It cannot arise from inequivalent sites or any effect other than the splitting of the levels of a single ion, as stress mixes the two states as well as splitting them [compare, for instance, (a) and (b) of Fig. 7]. However, let us ignore this difficulty for the moment and consider the effect of varying the direction of stress on the

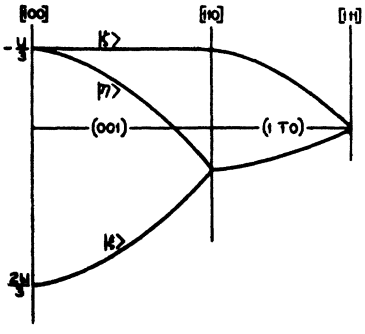

FIG. 8. Variation of the splitting of a T_2 state as the direction of applied stress is varied in the (001) and (110) planes, calculated on the assumption of a static Jahn-Teller distortion along [100]-type directions (note that u is negative for compressive stress).

[41] If by some quirk of the MgO lattice the orbital doublet were lowest, rather than the singlet, spin-orbit coupling would split it in first order into four Kramers doublets, giving four lines of equal intensity 30 cm^{-1} apart. This is not observed.

[42] In Moffitt and Thorsen's notation (Ref. 21), $\Delta = 3l_\epsilon^2/2\mu\omega_\epsilon^2$. From the stress splitting u we find the coupling parameter l_ϵ to be about 5000 cm^{-1}/Å, and taking $\hbar\omega_\epsilon$ as 200 cm^{-1}, μ as one oxygen mass, we find $\Delta \sim 1000$ cm^{-1}. It is therefore reasonable to attribute most of the bandwidth to the Jahn-Teller splitting.

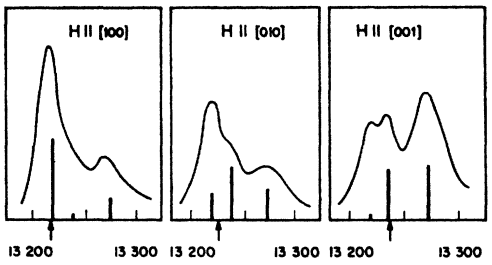

FIG. 9. Spectrograms for stress applied at 35° to [001] in the (001) plane. The vertical lines represent the relative line strengths predicted by the effective Hamiltonian theory of Sec. 6. The static Jahn-Teller effect would give a single line in each polarization, in the positions marked by the arrows.

spectrum. Stress along [001] obviously splits the three degenerate levels into a singlet and a doublet; while stress along [111], making equal angles with all three directions of distortion, can produce no splitting or polarization. The variation of the splitting as the direction of stress is varied from [100] through [110] to [111] is shown in Fig. 8. Here u has the same meaning as in the cubic case. The transition will be polarized according to the state involved; $H\|[100]$ induces transitions to $|\xi\rangle$, $H\|[010]$ to $|\eta\rangle$, $H\|[001]$ to $|\zeta\rangle$. For the particular case of a stress at $\cos^{-1}(1/\sqrt{3})(35°)$ to [100] in the (001) plane, we would expect three lines equally spaced and polarized parallel to [100], [010], and [001], respectively. Figure 9 shows that the observed effect of stress is quite different from this prediction. Measurements with the stress at 25° to [100] give a similar result.

Ham[14] has extended the theory of this section by allowing for overlap between the *vibrational* wave functions corresponding to the different directions of distortion. Each of the singlet electronic states brought lowest by the distortion is associated with a vibrational wave function u, which represents the lowest state of a two-dimensional harmonic oscillator displaced from the origin by the static Jahn-Teller distortion. A representative vibrational wave function u_1 (associated with $|^4T_2\xi\rangle$ is given approximately by

$$u_1=\frac{\pi}{\alpha^2}\exp-\frac{\alpha^2}{2}\{(q_1-a)^2+\tfrac{1}{3}(q_2-q_3)^2\}. \qquad (4)$$

Here a is the displacement in q_1 due to the Jahn-Teller distortion, and $\alpha^{-1}=(h/\mu\omega_\epsilon)^{1/2}$ is the rms zero-point displacement. The q's are defined in terms of normal coordinates in Table I(b). Matrix elements of operators connecting the different electronic states are reduced below their cubic values by $\langle u_1|u_2\rangle$, the overlap between the u's. Spin-orbit coupling has only off-diagonal matrix elements in the (ξ,η,ζ) basis, so the effective spin-orbit coupling parameter ($\zeta/6$ for the $^4T_2$ state in a cubic field) is reduced to $\langle u_1|u_2\rangle\zeta/6$. First-order spin-orbit splittings are reduced proportionally, though qualitatively they retain their "cubic" character. The same is true of operators transforming as T_2, such as [111] strain. We can estimate an upper limit for $\langle u_1|u_2\rangle$ from the observation that the splitting under the maximum [111] stress is less than 2 cm^{-1}, whereas that calculated neglecting Jahn-Teller effects is 8 cm^{-1} [see Fig. 6(c)]. Thus $\langle u_1|u_2\rangle<0.25$,[43] and we expect to find the first-order spin-orbit splittings in zero stress reduced from 30 and 50 cm^{-1} to less than 8 and 13 cm^{-1}, respectively. Second-order spin-orbit splittings are also considered by Ham; they are 2 cm^{-1} or less in the present case and can be neglected. Thus Ham's theory does not explain the 40-cm^{-1} splitting observed.

6. AN EFFECTIVE HAMILTONIAN

It will be shown in this section that it is possible to fit the results with an effective Hamiltonian containing terms of T_{2g} symmetry. Such noncubic terms, which simulate the effect of a local trigonal distortion, cannot occur in the true Hamiltonian (local deviations of the environment from cubic symmetry are known from spin-resonance to be extremely small[25]). A possible justification of this procedure, and a physical interpretation of the noncubic terms, will be left until later.

We take as our basis states $|\xi\rangle,|\eta\rangle,|\zeta\rangle$ transforming as yz,zx,xy. Each state is a product of the corresponding substate of the $^4T_2$ electronic level and a vibrational state with a wave function u such as is written down in Eq. (4), which represents the appropriate nuclear configuration ([100] distortion with $|\xi\rangle$, etc.).

Let us suppose that there are terms H_ξ, H_η, and H_ζ in the Hamiltonian which connect the basis states thus:

$$\langle\zeta|H_\xi|\eta\rangle=\langle\xi|H_\eta|\zeta\rangle=\langle\eta|H_\zeta|\xi\rangle=w/3. \qquad (5)$$

Under this perturbation, and in the absence of a stress, the effective Hamiltonian matrix is

$$\begin{Vmatrix} 0 & w/3 & w/3 \\ w/3 & 0 & w/3 \\ w/3 & w/3 & 0 \end{Vmatrix}.$$

Diagonalizing it we find that the threefold degenerate state splits into a doublet and a singlet, the former lowest for positive w. Despite a superficial resemblance, this splitting has nothing to do with tunnelling[24] or "inversion splitting."[44] Such splitting of a T state cannot occur in a cubic crystal.[14,23] The vibronic wave functions are:

$$\begin{aligned} &\text{Singlet,} && (1/\sqrt{3})(|\xi\rangle+|\eta\rangle+|\zeta\rangle); \\ &\text{Doublet,} && (1/\sqrt{2})(|\xi\rangle-|\eta\rangle), \\ & && (1/\sqrt{6})(2|\zeta\rangle-|\xi\rangle-|\eta\rangle). \end{aligned} \qquad (6)$$

The splitting between these states is w, which we put

[43] Making the (rather implausible) assumption that the vibrational wave functions of Eq. (4) hold in the region of overlap, we find

$$\langle u_1|u_2\rangle\sim\exp(-3\alpha^2a^2/4)=\exp(-\Delta/2\hbar\omega_\epsilon)\sim0.1.$$

[44] I. B. Bersuker, Zh. Eksperim. i Teor. Fiz. **43**, 1315 (1962) [English transl.: Soviet Phys.—JETP **16**, 933 (1963)].

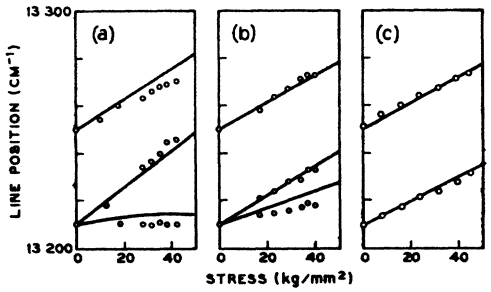

FIG. 10. Data of Fig. 6 compared with the predictions of Sec. 6: (a) $p\|[001]$; (b) $p\|[110]$; (c) $p\|[111]$.

equal to the observed splitting of 40 cm^{-1}. Remember that with each electronic component there is associated a corresponding distortion of the octahedron. In order to reproduce the experimental results we assume that the effect of stress can be included by taking matrix elements diagonal in the ξ,η,ζ representation to be the same as in the cubic case. We put all off-diagonal matrix elements equal to zero, that is, we neglect terms containing $\langle u_1|u_2\rangle$, the overlap of the vibrational wave function corresponding to different distortions. The use of the cubic diagonal matrix elements is reasonable as the static distortions associated with the Jahn-Teller effect are relatively small (of the order of 5%).[45]

The effective Hamiltonian for a general direction of stress with direction cosines (l,m,n) is

$$\begin{Vmatrix} (3l^2-1)u/3 & w/3 & w/3 \\ \cdots & (3m^2-1)u/3 & w/3 \\ \cdots & \cdots & (3n^2-1)u/3 \end{Vmatrix}. \quad (7)$$

The energy levels calculated from (7) are compared with the experimental results for [001], [110], and [111] stress in Fig. 10.[39] In Figs. 9 and 11, and in Table II, the calculated relative line strengths are compared with experiment for a number of different directions of stress.[46] In view of the fact that w is the only adjustable parameter, the agreement of the calculated energy levels with observation is remarkably good. The polarization data are in general qualitative agreement with prediction, but quantitatively there are some discrepancies. The polarization is never so strong as predicted, and this is understandable in view of the light scattering and consequent depolarization mentioned in Sec. 3. The lowest line of the group is sharper than the others and therefore tends to look stronger in the spectrograms than it really is. Furthermore, the method of separating partially resolved lines which was used to obtain the data in Table II tends to discriminate against weak and unresolved lines. This probably accounts for the apparent weakness of the middle line relative to the outer two. Apart from these sources of systematic error, random errors in the data of Table II amount to ± 0.05, except for the zero-stress data. The zero-stress data are averaged over a number of crystals and are accurate to ± 0.02; they do not suffer significantly from the systematic errors noted above.

TABLE II. Comparison of integrated line intensities with the predictions of the effective-Hamiltonian theory of Sec. 6. All data are normalized to unit total area, and (except for the zero-stress data) corrected to 40 kg/mm².

Stress direction	Polarization (H vector)	Lowest line Obs	Lowest line Calc	Middle line Obs	Middle line Calc	Upper line Obs	Upper line Calc
Zero stress	Unpol.	0.68	$\frac{2}{3}$	···		0.32	$\frac{1}{3}$
[001]	[100]	0.15	0.05	0.4	0.5	0.45	0.45
	[001]	0.7	0.9	0.05	0.0	0.25	0.1
[110]	[100]	0.6	0.5	0.15	0.27	0.25	0.23
	[001]	0.15	0	0.3	0.55	0.55	0.45
	[110]	0.6	1	0.1	0	0.3	0
25° to [100] in (001)	$\|p$	0.65	0.94	0.1	0.05	0.25	0.01
	$\perp p$ in (001)	0.3	0.01	0.4	0.50	0.3	0.49
	[001]	0.2	0.05	0.3	0.45	0.5	0.50
35° to [100] in (001)	[100]	0.65	0.73	0.05	0.05	0.3	0.19
	[010]	0.55	0.23	0.15	0.50	0.3	0.29
	[001]	0.2	0.04	0.3	0.45	0.5	0.52

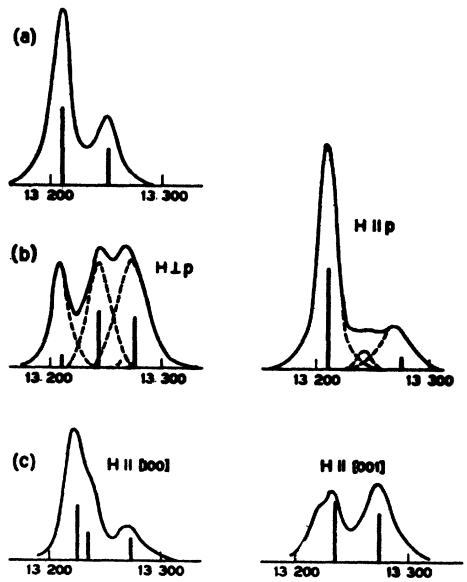

FIG. 11. Spectrograms of Fig. 7 compared with the predictions of Sec. 6. (a) zero stress; (b) $p|[001]$; (c) $p\|[110]$. No splitting or polarization is predicted, or observed, for [111] stress (see Figs. 7 and 10). The dotted lines in (b) indicate how a spectrogram is analyzed to obtain the data in Table III.

[45] Neglect of second-order effects that result from the mixing of cubic states by the large Jahn-Teller distortion can be justified as follows. Reduction of the local symmetry from O_h to D_{4h} splits the $^4T_2$ state into ^4E and $^4B_2$, and we are interested only in the $^4B_2$ (orbital-singlet) state. Since there is no other quartet state of this symmetry in the d^3 configuration, no other states are mixed with it by the distortion, and the second-order term vanishes. There are, of course, a number of third-order terms that contribute splitting up to 1 cm^{-1}; these have been neglected.

[46] Because Eq. (7) would lead to a polarized spectrum even in the absence of a stress, it is necessary to sum over four such matrices, obtained by changing the signs of off-diagonal elements in fours, in order to calculate the line strengths. Because T_2 operators are quenched, each state retains a fourfold degeneracy even under stress, and the energy levels are the same as for the 3×3 matrix (7).

The off-diagonal terms, H_ξ, H_η, and H_ζ, which we have introduced into the Hamiltonian can be given a simple physical interpretation. They are just what we would have if there were local static distortions oriented at random along [111]-type directions.[46] The Jahn-Teller effect, while sufficiently strong to reduce the splitting resulting from an externally applied [111] strain below the limit of observation, only partially quenches the effect of the much larger local trigonal distortion. These local distortions have two peculiar features: they are not present when the ion is in its $^4A_2$ ground state[25] or in the ^2E state[26]; and they are fixed in magnitude though varying in direction. The apparent distortion must be a consequence of the Jahn-Teller effect, presumably through interaction with τ_{2g} vibrations. Possibly these vibrations, whose interaction with the $^4T_2$ state is fairly strong (about $\frac{1}{3}$ the strength of the ϵ_g interaction) combine to produce a local static trigonal distortion. Such a distortion need not in fact be permanent; it need merely be "quasistatic," i.e., longlived compared to the lifetime of the $^4T_2$ state (about 10^{-12} sec).

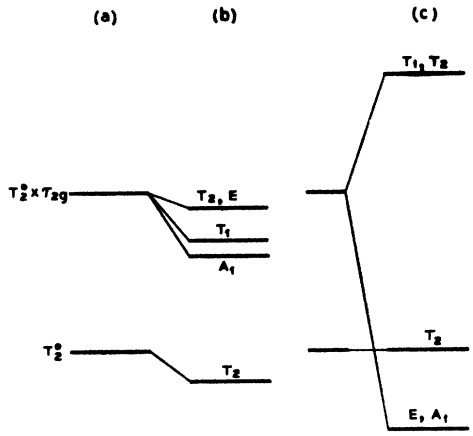

FIG. 12. Energy-level diagram for a T_2 electronic state interacting with τ_{2g} vibrations, in the presence of a large ϵ_g distortion due to the static Jahn-Teller effect. T_2^0 represents the vibronic states $(u_1\psi_\xi, u_2\psi_\eta, u_3\psi_\zeta)$, without τ_{2g} vibrations. A_2, E, T_1, T_2 are vibronic states resulting from the excitation of τ_{2g} vibrations. (a) No interaction; (b) weak interaction (second-order perturbation theory) according to Moffitt and Thorsen (Ref. 21); (c) interaction with the upper branch as described in the text.

7. DYNAMIC JAHN-TELLER EFFECT

To confirm the hypothesis made in the previous section, that interaction with τ_{2g} vibrations can lead to static or "quasistatic" trigonal distortion, would probably require a full calculation of the vibronic energy levels of an octahedral complex including all modes and allowing for anharmonicity. This would be extremely difficult[14,21,24] and has not been attempted. An alternative approach, which considers the properties of the vibronic levels which arise when a τ_{2g} vibration interacts weakly with the system, will be outlined in this section. The validity of the calculation is open to question as the results of perturbation theory are extended beyond their range of validity and many important terms are neglected. We find that there might in certain circumstances be a reordering of the vibronic energy levels, with the effect that the observed zero-stress splittings arise from cubic rather than noncubic terms in the Hamiltonian. Unfortunately it seems rather unlikely that such a reordering can occur in any physical situation. The purpose of this section is not so much to provide an explanation for the experimental results, as to illustrate a possible approach and to illuminate some of its pitfalls. Insofar as the effective Hamiltonian of the previous section describes the data correctly, its validity is independent of the particular model proposed to explain it.

First we must establish some notation. We use Van Vleck's normal coordinates $Q_1 \cdots Q_6$, which transform as shown in Table I(a). As before, it is convenient to use the linear combinations of Q_2 and Q_3 given in Table I(b); they are no longer orthogonal coordinates but they have an obvious symmetry lacking in Q_2 and Q_3. Ignoring terms in Q_1, the ground-state vibrational wave function in the vicinity of the Jahn-Teller minimum located a distance along the q_3 axis is

$$u_3 = \exp-[\tfrac{1}{2}\alpha_1^2(q_3-a)^2+\tfrac{1}{6}\alpha_2^2(q_1-q_2)^2 + \tfrac{1}{2}\alpha_3^2(Q_4^2+Q_5^2)+\tfrac{1}{2}\alpha_4^2Q_6^2]. \quad (8)$$

This is associated with the electronic state $|^4T_2\zeta\rangle$ whose wave function we write ψ_ζ. Similarly u_2 is associated with ψ_η, u_1 with ψ_ξ, and the ground-state vibronic wave functions transform as T_2 with components $(u_1\psi_\xi, u_2\psi_\eta, u_3\psi_\zeta)$. The α's are appropriate combinations of force constants and frequencies for the various vibrations. The distinctions between α_1 and α_2, and between α_3 and α_4, arise from anharmonic effects (variation of force constants with static distortion). In particular the distinction between α_3 and α_4 takes into account coupling between the ϵ_g and τ_{2g} modes. No important physical effects seem to follow from drawing these distinctions and for simplicity we will ignore them. Equation (8) then reduces to Eq. (4) when τ_{2g} vibrations are neglected.

Now let us excite one τ_{2g} vibration in this system. The angular parts of the three possible vibrational wave functions we call φ_ξ, φ_η, or φ_ζ, transforming as Q_4, Q_5, Q_6, respectively. The three vibrational states described by $\varphi_\xi, \varphi_\eta, \varphi_\zeta$ can be combined with the original vibronic triplet $u_1\psi_\xi, u_2\psi_\eta, u_3\psi_\zeta$ in a number of ways, but in the absence of interaction with τ_{2g} vibrations all the nine resulting states will be degenerate at $\hbar\omega_\tau$ above the ground state, $\hbar\omega_\tau$ being the energy of one τ_{2g} vibration. Such a ninefold degenerate level is represented by $T_2^0 \times \tau_{2g}$ in Fig. 12(a). Now assume a weak interaction between the T_2 vibronic state and the τ_{2g} vibration. To belong to the Hamiltonian of the crystal, the interaction must have over-all cubic symmetry and cannot split the lowest state T_2^0. On the other hand it will split

TABLE III. Wave functions of the states arising from $T_2^0 \times \tau_{2g}$.

A_1	$(1/\sqrt{3})[\psi_\xi u_1\varphi_\xi+\psi_\eta u_2\varphi_\eta+\psi_\zeta u_3\varphi_\zeta]$
E	$(1/\sqrt{6})[2\psi_\zeta u_3\varphi_\zeta-\psi_\xi u_1\varphi_\xi-\psi_\eta u_2\varphi_\eta]$
	$(1/\sqrt{2})[\psi_\xi u_1\varphi_\xi-\psi_\eta u_2\varphi_\eta]$
T_1	$(1/\sqrt{2})[\psi_\eta u_2\varphi_\zeta-\psi_\zeta u_3\varphi_\eta]$
	$(1/\sqrt{2})[\psi_\zeta u_3\varphi_\xi-\psi_\xi u_1\varphi_\zeta]$
	$(1/\sqrt{2})[\psi_\xi u_1\varphi_\eta-\psi_\eta u_2\varphi_\xi]$
T_2	$(1/\sqrt{2})[\psi_\eta u_2\varphi_\zeta+\psi_\zeta u_3\varphi_\eta]$
	$(1/\sqrt{2})[\psi_\zeta u_3\varphi_\xi+\psi_\xi u_1\varphi_\zeta]$
	$(1/\sqrt{2})[\psi_\xi u_1\varphi_\eta+\psi_\eta u_2\varphi_\xi]$

the $T_2^0 \times \tau_{2g}$ state into vibronic states of T_2, T_1, E, and A_1 symmetry, and a table of Wigner coefficients[47] tells us that these states have the wave functions given in Table III.

Of these wave functions, the E and A_1 contain only "diagonal" products like $\psi_\xi\varphi_\xi$, while T_1 and T_2 only contain "off-diagonal" products like $\psi_\xi\varphi_\eta$. Thus in the E and A_1 states the electronic state and the vibration are (in a sense) in phase, while in the other states they are out of phase. It is therefore not unreasonable to suppose that the E and A_1 states will move together, possibly being pushed down in energy by the interaction, while the T_1 and T_2 will under the same circumstances be (relatively) pushed up. This will be made more plausible by consideration of particular terms in the interaction later on. If the interaction is strong enough, the E and A_1 states can be pushed down below the T_2^0 "ground" state as illustrated in Fig. 12(c), and themselves become the lowest vibronic states in spite of containing admixtures of states with one or more quanta of τ_{2g} vibration. Once these vibronic states are well below all the others arising from the same electronic state they cannot decay except by change of electronic state, and hence become relatively sharp at low temperatures. On the other hand the "vibrationless" T_2 state, being no longer the lowest lying vibronic state, can dispose of energy by phonon emission and is broadened accordingly.

We now see that the E and A_1 states, which according to the above argument will be degenerate or nearly so, have just the same electronic parts as the zero-stress wave functions obtained from the effective Hamiltonian of the previous section. $\psi_\xi u_1\varphi_\xi$ corresponds to $|\xi\rangle$, $\psi_\eta u_2\varphi_\eta$ to $|\eta\rangle$ and $\psi_\zeta u_3\varphi_\zeta$ to $|\zeta\rangle$. However, it is no longer necessary to assume noncubic terms in the Hamiltonian in order to explain the zero-stress splitting; having different cubic representations the E and A_1 states can be split apart even in a cubic situation. The zero-stress splitting between E and A_1 arises from the fact that transitions between the basis states $|\psi_\xi u_1\varphi_\xi\rangle$, $|\psi_\eta u_2\varphi_\eta\rangle$, $|\psi_\zeta u_3\varphi_\zeta\rangle$ are now possible by virtual emission and absorption of τ_{2g} phonons.

[47] G. F. Koster, J. O. Dimmock, R. G. Wheeler, and H. Statz, *Properties of the 32 Point Groups* (MIT Press, Cambridge, Massachusetts, 1963).

Regarding the calculation of the effect of stress we can make the following observations. The shift in the vibrational energies due to strain will be small, or order $\hbar\omega\times$strain or less than 1 cm^{-1}. This justifies the consideration of only the electronic matrix elements of strain. Secondly, in the same approximation, the orthogonality of the φ's ensures that off-diagonal matrix elements of strain, such as $\langle\psi_\xi u_1\varphi_\xi|u_\zeta{}^{T_2}|\psi_\eta u_2\varphi_\eta\rangle$, are zero. It is not at all obvious how the observed lines acquire their intensity, which is within an order of magnitude of that to be expected for the magnetic dipole transition without any Jahn-Teller effect.[26] The magnetic-dipole operator transforms as T_{1g} and so cannot cause transitions between the $^4A_2$ ground state and pure E and A_1 states. Two possibilities arise; spin-orbit coupling may mix in enough of the higher states (the T_1 and T_2 states of Fig. 12, for instance) to produce the necessary intensity. Alternatively, a τ_{2g} vibration may be involved; though it is difficult to see in this case why the doublet shows all the characteristics of a no-phonon line (see Sec. 3). This problem needs further study.

Finally, we are concerned to make it plausible that the E and A_1 states can indeed lie well below the associated T_1 and T_2 states. The work of Moffitt and Thorsen[21] shows that, in the absence of ϵ_g distortion, weak interaction of a T_2 state with a τ_{2g} vibration produces the initial splittings shown in Fig. 12(b). A sufficiently strong interaction brings the lowest A_1 and T_2 vibronic states into coincidence but does not change the order of the states; this corresponds to a static Jahn-Teller distortion along (111) directions. Unpublished calculations by D. E. McCumber show that the Moffitt and Thorsen result still holds in the presence of ϵ_g distortion, *provided* one confines one's attention to the states $\psi_\xi u_1, \psi_\eta u_2, \psi_\zeta u_3$, i.e., to the lower branch (branch 2) of Fig. 1. The splittings are reduced by a factor $|\langle u_1|u_2\rangle|^2$ but the order of the states is unchanged.[48] If $\langle u_1|u_2\rangle$ is sufficiently small, however, a more important effect may be the mixing (by the τ_{2g} vibrations) of such states as $\psi_\eta u_1$ with $\psi_\zeta u_1$, i.e., mixing of branches 2 and 3 in Fig. 1. Such mixing can give rise to a variety of splittings, but under certain circumstances the E and A_1 states can be pushed down while the T_1 and T_2 states are either pushed up, or unshifted in second order [Fig. 12(c)]. The splitting is now of order $C_\tau{}^2/\Delta$, where C_τ is the coefficient of coupling to the τ_{2g} vibrations[49] and Δ the Jahn-Teller splitting (Fig. 1). From the stress splitting calculated in Sec. 4 we find $C_\tau\sim300$ cm^{-1}, and as $\Delta\sim1000$ cm^{-1}, $\hbar\omega_\tau\sim100$ cm^{-1}, a reordering of the energy levels is quite possible. We might expect the $E-A_1$ splitting w to be of order $\langle u_1|u_2\rangle C_\tau$, so taking the observed value of w (40 cm^{-1})

[48] This is simply a special case of the quenching of an off-diagonal operator, in this case interaction with τ_{2g} vibrations, discussed by Ham in Ref. 14.

[49] C_τ is related to the coupling coefficient l_τ of Ref. 21 by $C_\tau=l_\tau(h/\mu\omega_\tau)^{1/2}$. C_ϵ is defined analogously for ϵ_g distortion.

we find $\langle u_1|u_2\rangle \sim 0.13$, in agreement with the previous estimate.[43] Quite a small mixing (of order 10%) is sufficient to explain the reordering of the states, so the optical selection rules will not be drastically altered. Of course, by the time this reordering occurs, the states will no longer have the relatively simple wave functions of Table III, but will have acquired substantial admixtures of higher vibrational states. This will not, however, alter their electronic parts, nor the symmetry properties of their vibrational parts which continue to transform as Q_4, Q_5, Q_6, so the arguments of the section are unaffected. It is of interest to note that as $\Delta \sim C_\epsilon^2/\hbar\omega_\epsilon$, the condition for reordering of the states in Fig. 12 is $C_\tau^2/\hbar\omega_\tau \sim C_\epsilon^2/\hbar\omega_\epsilon$. This is essentially the condition that tetragonal and trigonal distortion compete rather closely to give the absolute minimum of energy.[5,21] While we know from experiment that in fact tetragonal distortion gives the absolute minimum, a relatively small change in parameters might well push us over into the trigonal regime.

Although perturbation theory, by the above argument, might be held to predict that the E and A_1 states can be brought lowest, we know that in both limits, τ_{2g} interactions very strong or very weak relative to ϵ_g interactions, the T_2 state is in fact lowest.[14,21] It seems improbable that in the intermediate situation this should not also be the case. F. S. Ham (private communication) has made a calculation using the nine states belonging to T_1 and T_2 in Fig. 12 as a basis. He finds that if the T_1 state is low enough (but not below the lowest T_2) he can reproduce the data, including the intensities, the states retaining a threefold vibrational degeneracy which is not raised by stress. It is necessary to suppose that $\hbar\omega_\tau$ is rather small (~ 40 cm^{-1}) for this approach to work, but the intensity problem is solved and no actual reordering of states is required. It is of interest to note that the mean values of the τ_{2g} coordinates, Q_4, Q_5, and Q_6, do not vanish in Ham's T_2 states, but are of the same order as their rms values α^{-1}. This is not the case for the E and A_1 states discussed earlier. It may be that this fact is related (though not in any very obvious manner) to the local trigonal distortion postulated in Sec. 6.

8. CONCLUSION

To summarize, we have shown that the Jahn-Teller effect occurs in the $^4T_2$ excited state of V^{2+} in MgO, but that it is more complicated than was previously to be expected. Whereas ϵ_g distortion is dominant in the nuclear configuration of the $^4T_2$ state, τ_{2g} vibrations also play an important role. An effective Hamiltonian successfully describes the lowest vibronic states and the effect of stress upon them, but the interpretation of this Hamiltonian in terms of more fundamental concepts is difficult. In particular, it is not at present clear whether the most fruitful theoretical approach is to try to explain the data in terms of static or "quasistatic" distortions as suggested at the end of Sec. 6, or to look at the properties of particular vibronic states as in Sec. 7. The author is content to leave that question as a challenge to the theorists, and to continue with experimental work on related systems.

ACKNOWLEDGMENTS

I am grateful to J. Ferguson, F. S. Ham, M. H. L. Pryce, R. Orbach, S. Sugano, and W. Thorsen, and especially to D. E. McCumber, for many helpful discussions; to F. S. Ham for communicating his work before publication; to K. A. Ingersoll for his careful work in preparing specimens and making most of the optical measurements; and to F. R. Merritt for making the spin-resonance measurement.